Article

Microrheology of Bacterial Biofilms In Vitro: *Staphylococcus aureus* and *Pseudomonas aeruginosa*

S. S. Rogers, C. van der Walle, and T. A. Waigh

Langmuir, **Article ASAP** • Publication Date (Web): 04 November 2008

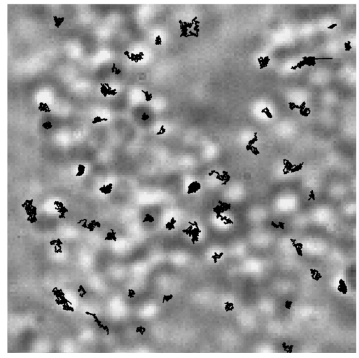

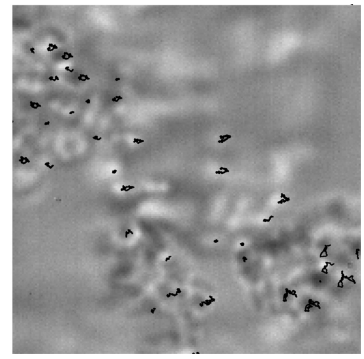

Microrheology of Bacterial Biofilms In Vitro: *Staphylococcus aureus* and *Pseudomonas aeruginosa*

S. S. Rogers,[†] C. van der Walle,[‡] and T. A. Waigh*,[†]

School of Physics and Astronomy, University of Manchester, Manchester M13 9PL, U.K., and University of Strathclyde, SIPBS, 27 Taylor Street, Glasgow G4 0NR, U.K.

Received July 29, 2008. Revised Manuscript Received September 28, 2008

The rheology of bacterial biofilms at the micron scale is an important step to understanding the communal lifecycles of bacteria that adhere to solid surfaces, as it measures how they mutually adhere and desorb. Improvements in particle-tracking software and imaging hardware have allowed us to successfully employ particle-tracking microrheology to measuring single-species bacterial biofilms, based on *Staphlococcus aureus* and *Pseudomonas aeruginosa*. By tracking displacements of the cells at a range of timescales, we separate active and thermal contributions to the cell motion. The *S. aureus* biofilms in particular show power-law rheology, in common with other dense colloidal suspensions. By calculating the mean compliance of *S. aureus* biofilms, we observe them becoming less compliant during growth, and more compliant during starvation. The biofilms are rheologically inhomogeneous on the micron scale, as a result of the strength of initial adhesion to the flow cell surface, the arrangement of individual bacteria, and larger-scale structures such as flocs of *P. aeruginosa*. Our *S. aureus* biofilms became homogeneous as a function of height as they matured: the rheological environment experienced by a bacterium became independent of how far it lived from the flow cell surface. Particle-tracking microrheology provides a quantitative measure of the "strength" of a biofilm. It may therefore prove useful in identifying drug targets and characterizing the effect of specific molecular changes on the micron-scale rheology of biofilms.

1. Introduction

Bacterial biofilms are communities of bacteria which adhere to solid surfaces. Many bacteria have the ability to live either in a planktonic or biofilm state, and may transit between either states following cues in the environment.[4,6,10,22,21] Well-studied species such as *Pseudomonas aeruginosa* exhibit quorum-sensing behavior during various parts of their life cycles, including attachment to and detachment from a surface.[15,26,34] While in a biofilm state, many bacteria produce an exopolysaccharide,[5,7,9] whose function is to bind together the bacterial cells, exclude viruses and antibiotics from the biofilm, and protect the biofilm from grazers and phagocytic cells.[3] As bacteria such as *P. aeruginosa* detach from a biofilm, they secrete enzymes to cleave the extracellular polymers.[2] The bacteria thus have the ability to modulate the mechanical properties of the biofilm according to the requirements of their colonial life cycles. Until now it has been difficult to measure the mechanical properties of bacterial biofilms as they grow and disintegrate, although we note the work of Stoodley et al.[16,32,31] who measured the approximate viscoelasticity and yield strength of biofilm flocs as they were deformed in shear flow, and Schofield et al.[28] who employed a quartz crystal microbalance to measure various properties of biofilms. We also note related studies of rheological and mechanical effects in biofilms: viscosity of reconstituted alginate gels,[11] diffusion of antibiotics,[13] and the physics and chemistry of biofilm adhesion.[17,19,39] Rheology at the micron scale is directly relevant to the rate of dissociation of bacteria from a biofilm and the resistance of the biofilm from mechanical damage.

Particle-tracking microrheology (PTM) relies on tracking the Brownian motion of particles embedded in a medium, in order to calculate the mechanical properties of the medium in the vicinity of the particles.[8,18,20,24,36,37] For micron-sized particles, PTM yields measurements of the shear modulus[20,37] or shear compli-

* Corresponding author. Address: University of Manchester, School of Physics and Astronomy, Manchester, M13 9PL, U.K. E-mail: thomas.waigh@manchester.ac.uk. Telephone: +44 161 3068881.

[†] University of Manchester.

[‡] University of Strathclyde.

(1) Adams, S.; Frith, W. J.; Stokes, J. R. *J. Rheol.* **2004**, *48*, 1195–1213.

(2) Boyd, A.; Chakrabarty, A. M. *Appl. Environ. Microbiol.* **Jul 1994**, *60*(7), 2355–2359.

(3) Boyd, A.; Chakrabarty, A. M. *J. Ind. Microbiol.* **1995**, *15*(3), 162–168.

(4) Costerton, J. W.; Cheng, K. J.; Geesey, G. G.; Ladd, T. I.; Nickel, J. C.; Dasgupta, M.; Marrie, T. J. *Annu. Rev. Microbiol.* **1987**, *41*, 435–464.

(5) Costerton, J. W.; Irvin, R. T.; Cheng, K. J. *Annu. Rev. Microbiol.* **1981**, *35*, 299–324.

(6) Dunne, W. M. *Clin. Microbiol. Rev.* **2002**, *15*(2), 155–166.

(7) Gacesa, P. *Microbiology* **1998**, *144*(Pt 5), 1133–1143.

(8) Gittes, F.; MacKintosh, F. C. *Phys. Rev. E* **1998**, *58*, R1241.

(9) Gotz, F. *Mol. Microbiol.* **2002**, *43*(6), 1367–1378.

(10) Hall-Stoodley, L.; Costerton, J. W.; Stoodley, P. *Nat. Rev. Microbiol.* **2004**, *2*(2), 95–108.

(11) Hanlon, G. W.; Denyer, S. P.; Olliff, C. J.; Ibrahim, L. J. *Appl. Environ. Microbiol.* **2001**, *67*(6), 2746–2753.

(12) Hobbie, E. K.; Lin-Gibson, S.; Kumar, S. *Phys. Rev. Lett.* **2008**, *100*(7), 076001.

(13) Jefferson, K. K.; Goldmann, D. A.; Pier, G. B. *Antimicrob. Agents Chemother.* **2005**, *49*(6), 2467–2473.

(14) Jones, D. A. R.; Leary, B.; Boger, D. V. *J. Colloid Interface Sci.* **1991**, *147*, 479–495.

(15) Kievit, T. R. D.; Gillis, R.; Marx, S.; Brown, C.; Iglewski, B. H. *Appl. Environ. Microbiol.* **2001**, *67*(4), 1865–1873.

(16) Klapper, I.; Rupp, C. J.; Cargo, R.; Purvedorj, B.; Stoodley, P. *Biotechnol. Bioeng.* **2002**, *80*(3), 289–296.

(17) Landry, R. M.; An, D.; Hupp, J. T.; Singh, P. K.; Parsek, M. R. *Mol. Microbiol.* **2006**, *59*(1), 142–151.

(18) Levine, A. J.; Lubensky, T. C. *Phys. Rev. Lett.* **2000**, *85*, 1774–7, One- and two-particle microrheology.

(19) MacKintosh, E. E.; Patel, J. D.; Marchant, R. E.; Anderson, J. M. *J. Biomed. Mater. Res. A* **2006**, *78*(4), 836–842.

(20) Mason, T. G.; Ganesan, K.; van Zanten, J. H.; Wirtz, D.; Kuo, S. C. *Phys. Rev. Lett.* **1997**, *79*, 3282–5.

(21) O'Toole, G.; Kaplan, H. B.; Kolter, R. *Annu. Rev. Microbiol.* **2000**, *54*, 49–79.

(22) Parsek, M. R.; Singh, P. K. *Annu. Rev. Microbiol.* **2003**, *57*, 677–701.

(23) Prasad, V.; Koehler, S. A.; Weeks, E. R. *Phys. Rev. Lett.* **2006**, *97*(17), 176001.

(24) Rogers, S. S.; Waigh, T. A.; Lu, J. R. *Biophys. J.* **2008**, *94*(8), 3313–3322.

(25) Rogers, S. S.; Waigh, T. A.; Zhao, X.; Lu, J. R. *Phys. Biol.* **2007**, *4*, 220–227.

(26) Sauer, K.; Camper, A. K.; Ehrlich, G. D.; Costerton, J. W.; Davies, D. G. *J. Bacteriol.* **2002**, *184*(4), 1140–1154.

(27) Savin, T.; Doyle, P. S. *Biophys. J.* **2005**, *88*(1), 623–638.

10.1021/la802442d CCC: $40.75
Published on Web 11/04/2008

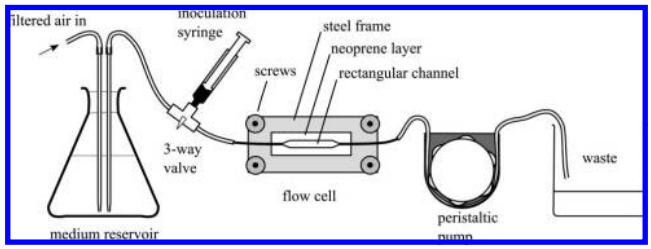

Figure 1. Biofilms were cultivated in a flow cell, consisting of a rectangular channel with tapered ends, cut into a Neoprene sheet, and sandwiched between a glass microscope slide and a coverslip in a rubber-padded steel frame. The biofilm was fed with a sterile aerated medium, using a peristaltic pump.

ance,[38] on the micron-scale, in the linear rheological limit. By tracking the motion of the bacteria themselves, which may be a combination of active and thermal motion, we have the opportunity of measuring the viscoelasticity seen by individual bacteria in the biofilm. This viscoelasticity may be a function of position in a heterogeneous biofilm, and of time during the development of the biofilm. Previous authors have studied the microrheology of thin films of protein at an air−water interface[23] and a fluid−gel interface.[12]

Here, we apply PTM to single-species biofilms composed of two different bacteria, both common opportunistic pathogens, which are capable of forming biofilms in their relationship with the human body. *Staphylococcus aureus* is a nonmotile spherical bacterium, common in the infection of wounds and medical implants. *P. aeruginosa* is a rod-shaped swimming bacterium, which, in its mucoid form, causes particularly problematic lung infections in cystic fibrosis patients.[10]

2. Experimental Section

2.1. Bacteria and Media. We used *S. aureus* strain FDA209 P variant (8588, NCIMB, Aberdeen, U.K.) and *P. aeruginosa* strain 217 M (received as a kind gift from Dr. Tyrone Pitt, Health Protection Agency, London, U.K.). The strains are of low and high mucoidy respectively. *S. aureus* was cultured in 25 g of LB-Miller medium (L3152, Sigma-Aldrich, Gillingham, U.K.) per liter of distilled, deionized water (Elga UHQ-PS-MK3, High Wycombe, U.K.). *P. aeruginosa* was cultured in King's A medium, consisting of 20 g of peptone (P1328, Melford Laboratories, Ipswich, U.K.), 10 g of glycerol, 10 g of anhydrous potassium sulfate, and 1.4 g of magnesium chloride per liter of distilled, deionized water. We also used M9 salts-only medium, consisting of 12.8 g of sodium phosphate dibasic, 3.0 g of potassium phosphate monobasic, 0.5 g of sodium chloride, and 1.0 g of ammonium chloride per liter of water. All reagents were obtained from Sigma-Aldrich except where specified. All media were sterilized by autoclave.

2.2. Cultivation of Biofilms. A purpose-built flow cell was constructed and set up as shown in Figure 1. The flow cell consisted of a long rectangular channel with tapered ends, cut out of a Neoprene sheet, of total dimensions $3 \times 7 \times 50$ mm^3, and volume of 1 mL. This sheet was sandwiched between a glass microscope slide and coverslip, which respectively formed the top and bottom of the flow cell. A steel frame held together the flow cell: the frame consisted of two rectangular plates, each padded by a thin sheet of rubber, with cut-out viewing windows, held together by a screw in each corner. In each experiment, a fresh coverslip was used, previously cleaned in a piranha solution. The flow cell and tubes were sterilized by pumping through first 10% Decon (Decon Laboratories, Ltd., Hove, U.K.), then 3% Virkon (Antec International, Sudbury, U.K.), then a 70% ethanol−30% water mixture, each for at least 15 min. This procedure was sufficient to ensure that no foreign organisms detectable by microscopy invaded the cultures.

Biofilm formation was initiated by inoculating the flow cell, which was preincubated at 37 °C, with a loading dose of overnight culture of each bacterium. The inocula had densities of approximately 8×10^8 cells/mL (*S. aureus*) and 6×10^8 cells/mL (*P. aeruginosa*); cell density was estimated by counting using a hematocytometer. The inoculum remained at rest in the flow cell for 1 h before being purged with fresh medium at a rate of 3 mL/min for 5 min. The purge ensured that only bacteria that had adhered to the surfaces remained, as observed by microscopy. The medium was then pumped at a steady flow rate of 0.2 mL/min to feed the biofilm. This flow has a Reynolds number of approximately 30. The flow was laminar, as seen in the microscope by the uniform drift of planktonic bacteria throughout the channel. The dilution rate of 0.2/min (i.e., residence time of 5 min) was high enough to ensure that planktonic bacteria were continuously washed out.

In each experiment, the medium was aerated by filtered air during biofilm growth, ensuring that an abundance of oxygen was supplied to the bacteria. Flow was maintained using a Bio-Rad EP-1 peristaltic pump (Bio-Rad, Hercules, CA) in all experiments.

Before applying PTM, we made several time lapse videos of biofilms forming from each species, in order to check the timescales of their growth and reproducibility of their behavior.

2.3. Starvation of Biofilms. After cultivating biofilms as above, the biofilms were starved by replacing the medium with M9 (salts only), keeping the flow rate at 0.2 mL/min. M9 and LB-Miller have similar osmolarities of 257 mOsm and 396 mOsm, respectively (measured with a Vitek Advanced Osmometer, model 3D3).

2.4. Microscopy. The flow cell was mounted in an Olympus IX71 inverted microscope with a condenser and 100× oil-immersion objective lens, enclosed in an environmental chamber heated to 37 °C. In all experiments, the condenser aperture was kept fully open. Images were captured each hour in bright-field mode, using a Photron Fastcam PCI camera (Photron (Europe) Ltd., Bucks, U.K.); during this time the peristaltic pump, heater, and air pump were briefly switched off to avoid vibrations. Framerates of 500−3000 s^{-1} were employed. The micrometre focusing scale on the microscope allowed us to scan vertically through the biofilm manually, examining planes 5 ± 1 μm apart. This distance is significantly greater than the vertical focusing depth of a single bacterium of approximately 2 μm: all bacteria in focus at one plane were invisible at the planes 5 μm distant; i.e., we are confident that the PTM methodology was not compromised by erroneous tracking of cells from adjacent bacterial layers. The light source was switched off to avoid sample damage when images were not being collected.

Time-lapse videos of growing biofilms were captured by mounting the flow cell in a Nikon TE2000 inverted microsope, with a 10× objective lens, in bright field mode with a very low light intensity. The microscope was enclosed in an environmental chamber heated to 37 °C and images were captured at 60 s intervals.

2.5. Particle Tracking. We tracked the motion of individual bacteria using our recently developed method: the polynomial-fit, Gaussian-weight algorithm (PFGW).[25] This allows us to accurately track the extrema of intensity corresponding to individual bacteria, without errors due to the presence of their neighbors in the image. Thresholds of acceptable eccentricity, radius, skewness, and particle lifetime were employed to reject intensity extrema that did not correspond to bacteria. Below we show example tracks and discuss the precision of the measurements.

2.6. Static and Dynamic Errors. In particle tracking, static error is the error in the measured position of a particle due to noise in the image, caused by ambient vibrations and fluctuations in light intensity or in the camera electronics.[27,33] In our previous publication,[25] we examined the relationship between static error and noise for particles

(28) Schofield, A. L.; Rudd, T. R.; Martin, D. S.; Fernig, D. G.; Edwards, C. *Biosens. Bioelectron.* **2007**, *23*(3), 407–413.
(29) Sollich, P. *Phys. Rev. E* **1998**, *58*, 739–759.
(30) Sollich, P.; Lequeux, F.; Hebraud, P.; Cates, M. E. *Phys. Rev. Lett.* **1997**, *78*, 2020.
(31) Stoodley, P.; Cargo, R.; Rupp, C. J.; Wilson, S.; Klapper, I. *J. Ind. Microbiol. Biotechnol.* **2002**, *29*(6), 361–367.
(32) Stoodley, P.; Lewandowski, Z.; Boyle, J. D.; Lappin-Scott, H. M. *Biotechnol. Bioeng.* **1999**, *65*(1), 83−92.

tracked using the PFGW method, finding that it followed the prediction of Thompson et al.[33] for errors dominated by background noise, i.e., a linear relationship between the root-mean-square error in distance ε_{RMS}, and the noise-to-signal ratio *N*/*S* at the particle peak. To evaluate the static error in the present study, we first measured the apparent displacements of 0.5 μm polymer beads (23579, Polysciences, Inc., Warrington, PA) dried onto a coverslip, capturing videos at 1000 fps using the 100× lens of our Olympus IX71 microscope. We gradually varied the light intensity between videos to change the *N*/*S*. The static error was calculated from the apparent displacements Δr of the beads, as $\varepsilon_{RMS} = (\langle|\Delta r|^2\rangle)^{1/2}$. Note that the static error has no time dependence, because the fluctuations that cause it are uncorrelated between frames. For each particle, the noise *N* was taken as the standard deviation of the intensity at the pixel nearest the particle peak, and the signal was taken as the difference between the peak and background intensities for the particular particle, calculated by $S = JR^2$, where *J* is the determinant of the matrix of second-order polynomial coefficients of the fit at the particle peak, defined in ref 25, and *R* is the radius. The same measures of *N* and *S* were applied to the biofilm images to study the significance of static errors in tracking bacteria.

Dynamic error is the error due to the movement of a particle during the finite exposure time of a single frame, i.e., "motion blur".[27] To minimize dynamic error, the exposure time was set to a quarter of the time interval between frames.

3. Results

We cultivated *S. aureus* and *P. aeruginosa* in the flow cell at 37 °C, feeding and washing out the planktonic bacteria continuously with a nutrient medium, and observed the biofilm forming on the glass coverslip that formed the bottom of the cell. Time lapse videos of each bacterium are included in the Supporting Information (SI). The behavior of *S. aureus* was relatively simple, and qualitatively reproducible. As the bacteria multiply, the biofilm covered the surfaces and thickened monotonically (SI Video 1). However, the *S. aureus* biofilms were not completely homogeneous: irregularly shaped voids were apparent on the glass at the base of the biofilm (Figure 2a). The voids do not seem to move or change with time but simply appear as the biofilm grows (see SI Video 1). We note that similar structures are described in the literature as "voids" and "channels".[26,34]

P. aeruginosa exhibited very different, and much less reproducible behavior. We observed that the bacteria changed their behavior erratically in the first 2 h after inoculation and the onset of flow: they adhered and detached from the surface, and changed in motility (SI Video 2). Large flocs of *P. aeruginosa* tended to form within 2 h, which were loosely attached or unattached to the glass surface (Figure 2b). (These flocs are variously named cell clusters, microcolonies, and mushrooms elsewhere.) Invariably, after 3 h from the start of the nutrient flow, only a small portion of the glass surface was covered by bacteria: large areas were entirely free of any adherent matter that could be resolved in the microscope.

By imaging the bacteria at high magnification each hour after the onset of the flow, at a range of heights above the glass surface, we could track the motion of individual bacteria at short timescales, as detailed in the Experimental Section. Figure 2c,d shows tracks of individual bacteria of both species. Note that only a small subset of the bacteria are tracked, because we reject particles that are too eccentric, skewed, large, or small, or which are not continuously tracked for more than 300 frames. The latter condition seems to be a strong criterion for rejecting spurious particles. The tracks of *S. aureus* appear as random walks, while those of *P. aeruginosa* show nonrandom motion such as directed swimming or circular motion on the surface.

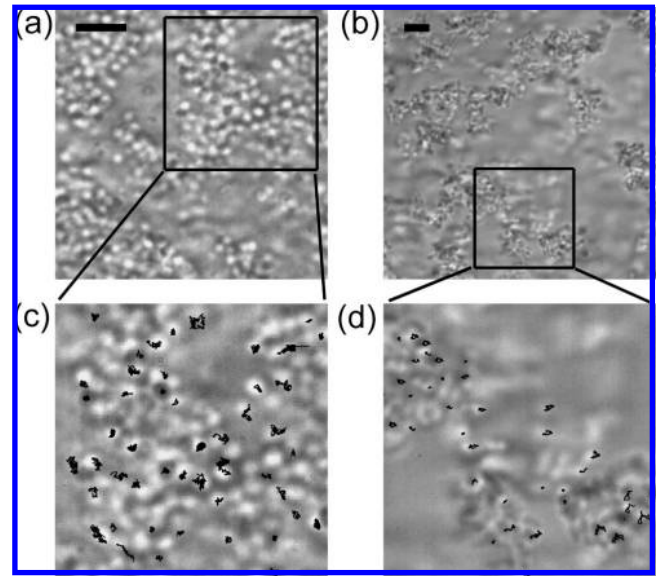

Figure 2. *S. aureus* (a) and *P. aeruginosa* (b) biofilms, after incubation times of 8 and 3 h, and heights of 0 and 10 μm from the flow cell surface, respectively. A portion of each image is magnified, and bacteria tracks are superposed (c,d). *S. aureus* formed spatially continuous biofilms with irregularly shaped holes, while *P. aeruginosa* formed irregularly shaped flocs. 5 μm scale bars are shown.

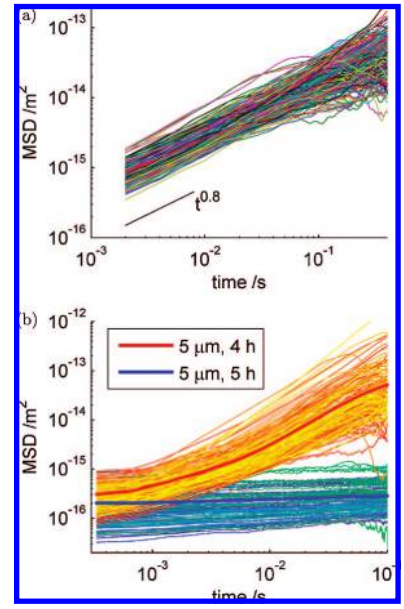

Figure 3. Example MSDs of individual bacterium tracks in biofilms of *S. aureus* (a) and *P. aeruginosa* (b), both at a height of 5 μm and at ages of 8 h and 4−5 h respectively. *S. aureus* shows power-law rheology over more than a decade of *t*, with various exponents, while *P. aeruginosa* (4 h) shows both active motion (swimming) at large *t* and thermal motion at small *t*. After the flow is ceased for 1 h (total 5 h), only thermal motion remains: the MSD now shows a slight power law dependence on *t*.

The mean square displacement in time *t* of each tracked bacterium was calculated according to $\mathrm{MSD}(t) = \langle|\Delta r(t)|^2\rangle$, where Δr is the displacement of the bacterium in the corresponding time. The theory of PTM is explained in ref 37. Examples are shown in Figure 3 for the two species. *S. aureus* displays only subdiffusive motion: the gradient of the MSD on the logarithmic plot is never greater than unity. Most individual tracks and the

(33) Thompson, R. E.; Larson, D. R.; Webb, W. W. *Biophys. J.* **2002**, *82*(5), 2775–2783.
(34) Tolker-Nielsen, T.; Brinch, U. C.; Ragas, P. C.; Andersen, J. B.; Jacobsen, C. S.; Molin, S. *J. Bacteriol.* **2000**, *182*(22), 6482–6489.

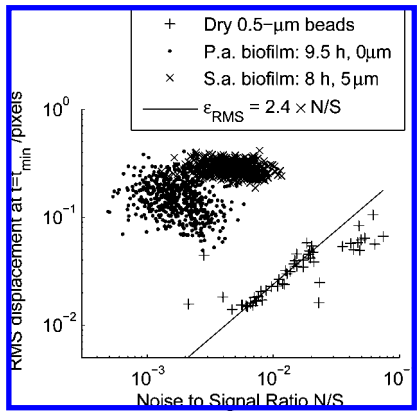

Figure 4. The dependence of root-mean-square (rms) displacement, at the shortest time scale, on *N*/*S*, for dry polymer beads and *S. aureus* and *P. aeruginosa* biofilms. For dry beads, rms displacements follow a model for the static error of position measurements;[33] however rms displacements of the bacteria are a factor of 10−100 higher, showing that static error is insignificant compared to real motion.

mean of all tracks show a power law MSD $\sim t^{\alpha}$ with $0 < \alpha \leq 1$. The biofilm is locally inhomogeneous: the MSD of neighboring bacteria differ by up to a factor of 10.

P. aeruginosa showed both superdiffusive and subdiffusive motion: the MSD is reminiscent of our previous study of intracellular particles in *Amoeba proteus*.[24] In most cases, motion was dominated by active motility of the bacteria: MSD $\sim t^{\alpha}$ with $1 < \alpha \leq 2$. By stopping the nutrient flow for 1 h, the bacteria were deprived of oxygen or nutrients, and the active motion ceased (Figure 3b). Thermal motion remained, and we can discern a slight power-law dependence of the MSD on t. It is apparent from Figure 3b that the change of slope at the shortest timescales ($t < 1$ ms) of the MSD for the well-fed *P. aeruginosa* corresponds to thermal motion. It could also be indicative of a static error in the measurement of particle position. Therefore we examine that possibility here in order to understand the limitations of the technique in measuring biofilm rheology.

To study the present significance of static error, we calculated the noise-to-signal ratio *N*/*S* of the images of tracked bacteria in the biofilms, and compared them with immobilized 0.5 μm polymer beads on a coverslip and the theory of Thompson et al.[33] Figure 4 shows the relationship between *N*/*S* and root-mean-square displacement at the shortest time scale (i.e., a single frame), for polymer beads and both species of bacteria. Each measured particle is represented as a single point on the graph. The apparent displacements of the polymer beads clearly follow a linear relationship $\varepsilon_{RMS} = cN/S$, where $c = 2.4$ here. Since we are using a different tracking method and different definitions of noise and signal than Thompson et al., we are not surprised that c differs slightly from their prediction. However it is still a constant of order unity, and is therefore in good agreement with their theory. The displacements of the bacteria are, in both cases, factors of 10−100 larger than the expected static error, according to the same relationship, and neither show a linear dependence. We therefore conclude that the measured displacements are dominated by real motion, and static error can be neglected. It is also apparent from Figure 3 that the MSD in both cases is dependent on time, unlike static error. Even in the starved *P. aeruginosa* of Figure 3, there is a steady dependence of MSD on time, over almost two decades of t, which is uncharacteristic of static error. By calculating *N*/*S*, we found that the expected static error was much less than the measured displacements at heights of up to approximately 30 μm in all biofilms of total thickness of $\lesssim$60 μm. As biofilms grew thicker, we noticed the contrast and light intensity in the image decreasing, until a noticeable static error could be seen in the MSD at the shortest timescales. Thus we were limited to relatively thin biofilms, roughly the first 10 h of growth of *S. aureus* biofilms under our experimental conditions.

Since the *S. aureus* Biofilm is fairly uniform (apart from gaps) and displays no active motion, tracking its development as a function of incubation time and height above the surface is straightforward using PTM. Both the shear modulus and the shear compliance can be calculated from the mean square displacement.[37,38] We calculate the shear compliance $J(t)$ since it is more directly related to the measurements, being simply proportional to the MSD:

$$J(t) = \frac{3\pi a}{2k_B T}\mathrm{MSD}(t) \qquad (1)$$

where $a = 0.64$ μm is the radius of the *S. aureus* cell, measured from the captured images, k_B is Boltzmann's constant, and T is the absolute temperature. This equation describes perfect spheres, therefore a should be regarded here as the hydrodynamic radius of the bacteria. It also assumes the medium around the particle is homogeneous, and ignores the hydrodynamic interactions between bacteria and between each bacterium and the surface. Clearly the medium around each bacterium is locally very inhomogeneous. Thus, values of J obtained below should be regarded as the "effective compliance" experienced by each bacterium; i.e., the bacterium moves as if it were in a homogeneous medium of compliance J. This effective compliance represents the average rheology of the local environment, including neighboring bacteria, the medium between bacteria, and the presence of the solid surface.

We plot the mean compliance over all tracked bacteria $J_{mean}(t)$, as a function of height above the glass and incubation time in Figure 5. The number of tracked bacteria in each video is on the order of 100−1000; thus the counting error in the calculation of the mean is insignificant. The biofilm is softer (more compliant) at greater (compared to lesser) heights above the glass surface, although this difference decreases with increasing incubation time. After 5 h, the mean compliance is nearly independent of height above the surface. We can also examine the heterogeneity of the biofilm by fitting a power law $J = \beta t^{\alpha}$ to the compliance of each tracked bacterium, in the time range $10 \leq t \leq 100$ ms, and then plotting histograms of the exponent α and the reference compliance $J(t_{ref})$ at a reference time scale $t_{ref} = 10$ ms. These are shown for the same biofilm in Figure 6. We see that, as the biofilm grows, it becomes more homogeneous in terms of both exponent and reference compliance. At 0 μm we see the tail of the distribution at low compliance gradually disappear. This is caused by the bacteria that initially bind to the surface tightly, desorbing over approximately 4 h. This effect is not seen at greater heights above the flow cell surface.

The results for the *S. aureus* Biofilm above were qualitatively similar when the experiment was repeated twice more. In Figure 7 we show the exponent (a,c,e) and reference compliance (b,d,f) for each biofilm, as a function of incubation time and height above the glass. In each instance of the experiment (a,b, c,d, and e,f), the compliance becomes more uniform as a function of height, and tends toward a steady value of reference compliance and exponent, although this differed between each film. α tended to steady state values in the range 0.7−0.95, and $J_{mean}(t_{ref})$ tended to 1−4 m^2 N^{-1}.

Similarly, we used PTM to track the development of *P. aeruginosa* biofilms, as a function of incubation time and height above the surface. Unfortunately, the experiments were complicated by the heterogeneity of the biofilm, which consisted of

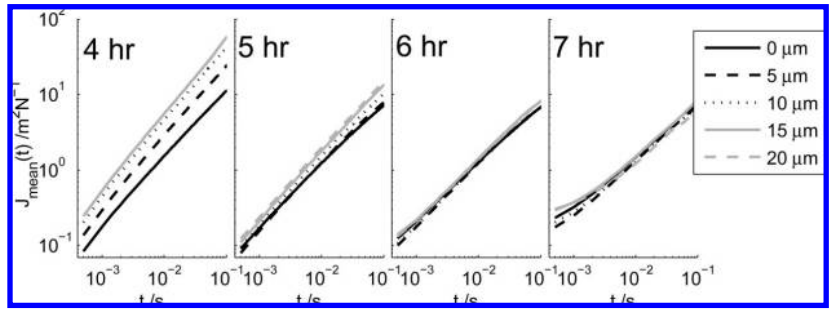

Figure 5. Mean shear compliances of an *S. aureus* biofilm, as a function of height from 0 to 20 μm and incubation time from 4 to 7 h. The compliances depend on t as power laws, with an exponent that decreases with incubation time. As they grow, the compliance also becomes more homogeneous with respect to the height above the flow cell surface.

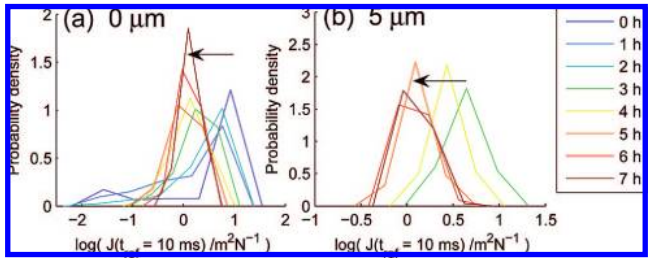

Figure 6. Histograms of a reference value of the compliance measured for individual bacteria in an *S. aureus* biofilm, at a height of 0−5 μm (a,b), and incubation times of 0−7 h. As the biofilm develops, we see the distribution of $\log(J(t_{ref}))$ changing in both shape and position. At both 0 and 5 μm, we see the peak of the distribution shift to lower values of compliance as incubation time increases. At 0 μm we see that the tail of the distribution at low compliance gradually disappears; this is caused by the desorption of bacteria that initially bind tightly to the surface. The arrows correspond to the direction of evolution of the main peak of J.

irregularly shaped flocs. Figure 8a shows mean compliance of a *P. aeruginosa* biofilm, at a range of heights, after 3 h of incubation. We examine the heterogeneity in microrheology with respect to position in the flocs in Figure 8b, by highlighting the bacterial tracks according to a reference value of the compliance, $J(t_{ref} = 1$ ms), in the subdiffusive regime. The distribution of compliances (shown as a histogram in Figure 8c) shows a main peak with several outliers: many bacteria experiencing high compliance are located on the edges of the flocs. Figure 9 shows $J_{mean}(t_{ref} = 1$ ms) and α fitted in the subdiffusive regime ($t \leq 2$ ms), for two instances of the experiment. Both $J_{mean}(t_{ref})$ and α vary erratically but remain in the approximate range $0.1 \leq J_{mean}(t_{ref}) \leq 0.5$ m^2 N^{-1} and $0 \leq \alpha \leq 0.5$. We believe the absence of reproducible trends is caused by a different portion of the biofilm appearing in the field of view at each time interval, because the flocs are continuously twitching under their own motility and drifting in the flow.

Having grown biofilms with constant feeding, we investigated their rheology as they disintegrated upon starvation. We cultivated two *S. aureus* biofilms as above for 10 h, then observed them disintegrating at 21 °C under a steady flow of M9 medium (salts only, without a carbon source). In both instances, the biofilms softened overall, with both $J_{mean}(t_{ref})$ and α increasing with time. α had reached 1 in the upper layers within 24 h, showing that the top of the Biofilm was fully eroded (Figure 10). $J_{mean}(t_{ref})$ and α simultaneously increased throughout the biofilm at all levels; evidently, the biofilm was softening everywhere, not just being eroded at the exposed top surface.

4. Discussion

We have seen that PTM allows us to measure the rheological environments of individual bacteria in biofilms grown in vitro, by employing our recently developed tracking algorithm.[25] Nonmotile *S. aureus* cells were easier to measure and interpret than motile *P. aeruginosa* cells, although we could distinguish both thermal and active motion in the latter, with the aid of a fast camera. The biofilms were locally inhomogeneous in the sense that the rheological environments of individual bacteria differed. However, by examining the mean and distribution of rheological measurements on sampled bacteria, clear trends of the changing rheology, as biofilms grew and disintegrated, emerged in *S. aureus*. Unfortunately, no such trends appeared in *P. aeruginosa* biofilms, because of added complications, such as the presence of flocs that are large on the scale of the microscope field of view, and gradually move under their own motility and the flow of the medium.

In both *S. aureus* and *P. aeruginosa* biofilms, we saw power-law rheology over 1−2 decades of time scale, i.e., a dependence $J \propto t^{\alpha}$ where $0 < \alpha < 1$. This type of rheology is strikingly reminiscent of colloidal microgels, and other "soft glassy" systems.[14,29,30] A general theory of these systems, based on simplified phenomenology, has been formulated by Sollich et al.,[29,30] and successfully predicts power-law rheology in the linear regime. Previous experiments on concentrated suspensions of hard spheres are perhaps more directly relevant to our biofilms: Jones et al.[14] found power-law rheology that sharply decreased in exponent from 1 to 0, as the packing fraction ϕ increased from 0.6 to 0.7. These fractions can be compared with the crystalline close packed fraction $\phi = 0.74$ and packing fractions of disordered jammed spheres at a range of $\phi < 0.74$: in particular, $\phi = 0.64$ for the "maximally random jammed" state.[35]

Thus, to some extent, we propose that bacterial biofilms resemble jammed hard spheres, especially for *S. aureus*, which is spherical, nonmotile, and, in the case of our strain, does not produce significant amounts of exopolysaccharides. Additional features of bacteria that may complicate the rheology are nonspherical morphology, size variation, deformability,[1] motility, adhesion, and exopolysaccharides. Unfortunately, it is not trivial to measure the packing fraction in the biofilms, even though we can observe and track individual bacteria. This is because it is difficult to distinguish all bacteria clearly enough to count them and measure their sizes: this leads to a large error in calculating ϕ.

(35) Torquato, S.; Truskett, T. M.; Debenedetti, P. G. *Phys. Rev. Lett.* **2000**, *84*(10), 2064–2067.
(36) Tseng, Y.; Kole, T. P.; Wirtz, D. *Biophys. J.* **2002**, *83*(6), 3162–3176.
(37) Waigh, T. A. *Rep. Prog. Phys.* **2005**, *68*(3), 685–742.
(38) Xu, J.; Viasnoff, V.; Wirtz, D. *Rheol. Acta* **1998**, *37*, 387–398.
(39) Ymele-Leki, P.; Ross, J. M. *Appl. Environ. Microbiol.* **2007**, *73*(6), 1834–1841.

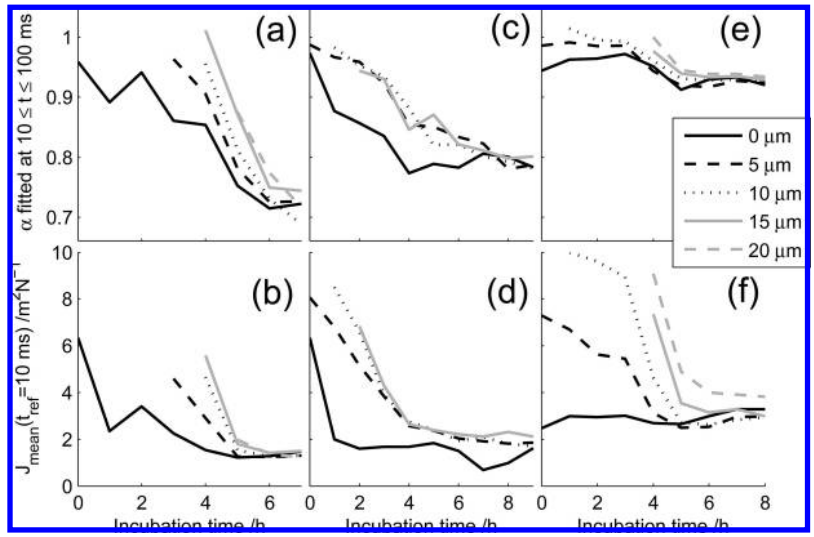

Figure 7. Mean rheology of developing *S. aureus* biofilms, showing exponent (a,c,e) and reference compliance (b,d,f) for each biofilm, as a function of incubation time and height above the glass. In each instance of the experiment (a,b, c,d, and e,f), the compliance becomes more uniform as a function of height, and tends toward a steady value of $J_{mean}(t_{ref})$ and α, although this differs between each instance. (Note that where bacteria are entirely absent, there are no data points, as in these experiments at greater heights and earlier times. No truncation or omission is made.)

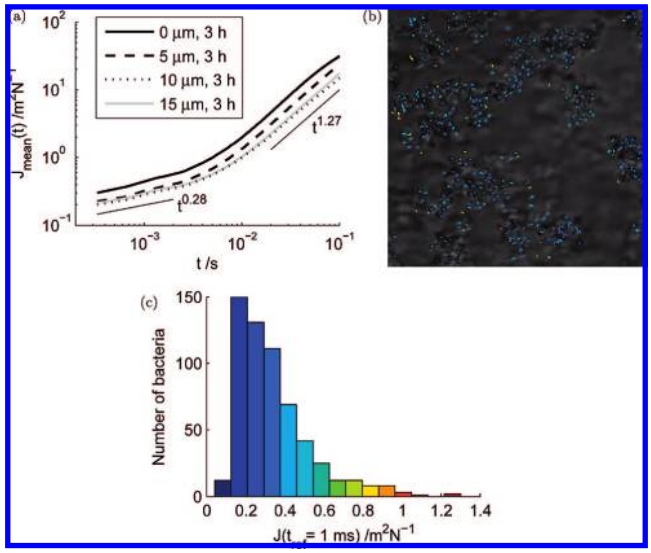

Figure 8. (a) Mean compliance of a 3 h *P. aeruginosa* biofilm as a function of depth. The compliance shows power law rheology at short timescales, with an exponent of ~0.28. (b) A micrograph of the biofilm at a height of 10 μm showing heterogeneous flocs: tracks of bacteria are superposed, colored according to $J(t_{ref} = 1\ ms)$, with colors corresponding to the histogram in (c). Many bacteria experiencing high compliance were located on the edges of flocs.

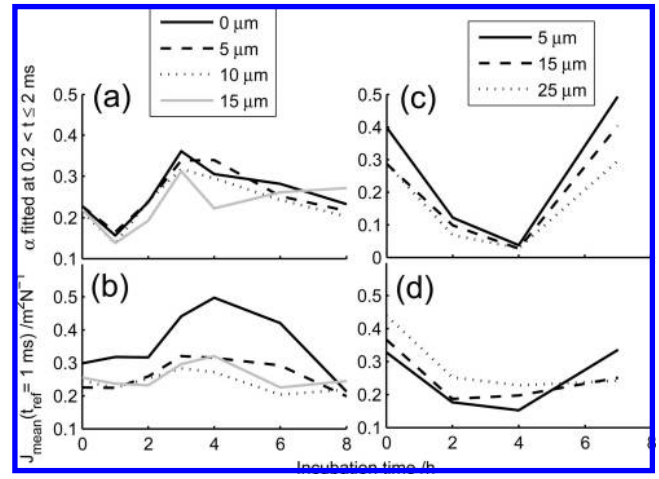

Figure 9. Mean rheology of developing *P. aeruginosa* biofilms, showing the exponent α in the subdiffusive regime, and the reference compliance $J(t_{ref} = 1\ ms)$. Two instances of the experiment are shown: (a,b) and (c,d). Unlike the mean rheology of *S. aureus* above, no trends are seen, due to the heterogeneity of the Biofilm and the movement of the flocs. However, measurements remain in the approximate ranges: $0.1 \leq J_{mean}(t_{ref}) \leq 0.5\ m^2\ N^{-1}$ and $0 \leq \alpha \leq 0.5$.

The *S. aureus* biofilms harden as they grow, with the power-law exponent and reference compliance both decreasing toward steady state values. The shear compliance is of order 1 $m^2\ N^{-1}$ at $t = 10$ ms; this value may be compared to water, with a compliance of $t/\mu = 10\ m^2\ N^{-1}$ where $\mu = 0.001$ Pa s, the viscosity of water. Therefore, at this time scale, the biofilm is approximately 10 times less compliant than water. It is interesting that the steady state rheology is independent of height above the flow cell surface: apparently the bacteria do not "feel" how far they are from the flow cell surface: even the bacteria touching the flow cell surface experience the same mean compliance as the bacteria above. This observation suggests that, in the mature biofilm, the bacteria do not stick to the surface any more tightly than they stick to each other. The early biofilm is different. We saw in Figure 6 that, at early times, some bacteria are tightly bound to the surface, although these detach within approximately 4 h. The underlying molecular mechanisms governing cell adhesion to the glass surfaces, and subsequent bacterial layers in the biofilm, are outside the scope of this paper. However, to our knowledge, the adherence of the bacteria to the glass surface will depend on nonspecific physical interactions and adhesion mediated via secreted exopolysaccharide. We also measured the softening of *S. aureus* biofilms as they starved in a medium with no carbon source. The power-law exponent and reference compliance both increased with time: the biofilms had mostly disintegrated within 24 h.

Although we did not obtain useful results on the development of *P. aeruginosa* biofilms, we see from their scaling exponents of the compliance $0 < \alpha < 0.5$ that they are much more solid-like than *S. aureus*. This may be because *P. aeruginosa* is rod-shaped and therefore will pack differently to a spherical bacterium, or because the adhesion is different: our strain of *P. aeruginosa* produces a large amount of exopolysaccharides. It may be possible

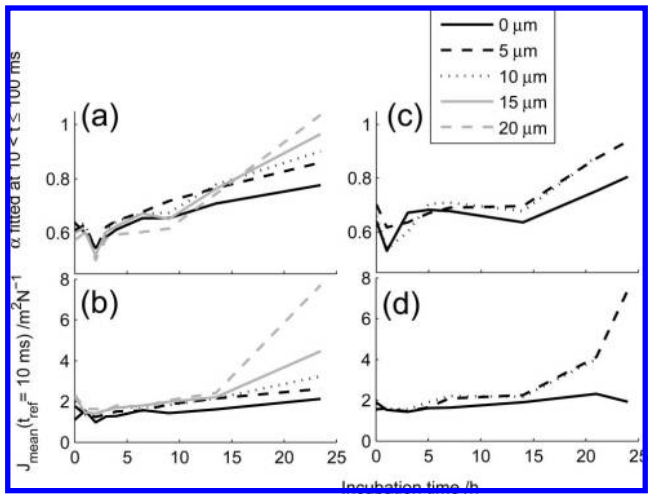

Figure 10. Mean rheology of starving *S. aureus* biofilms, showing exponent (a,c) and reference compliance (b,d) as a function of incubation time and height above the glass. In each instance of the experiment (a,b; c,d), the compliance becomes less uniform as a function of height, The biofilms soften overall, with both $J_{mean}(t_{ref})$ and α increasing with time.

to use PTM to monitor the development of *P. aeruginosa* biofilm flocs by immobilizing them, e.g., by exploiting their specific adhesion to a mucin-coated surface.[17]

We found that PTM is applicable to biofilms in the early stages of their formation, when they are relatively transparent: we could measure approximately 30 μm in each biofilm of total thickness less than around 60 μm. Thicker biofilms are not practical to measure by PTM because of the difficulty of tracking the individual cells by direct microscopy. However, it is likely that optical coherence tomography could provide analogous measurements in thicker biofilms.

5. Conclusion

The rheology of bacterial biofilms at the micron scale is an important step to understanding the communal lifecycles of bacteria, as it measures how they bind together and dissociate. Improvements in particle-tracking software and imaging hardware have allowed us to successfully employ PTM to measuring the microrheology of single-species bacterial biofilms, based on *S. aureus* and *P. aeruginosa*. The biofilms show power-law rheology, in common with other dense colloidal suspensions and soft glassy materials. By calculating the mean compliance of *S. aureus* biofilms, we observe them hardening during growth, and softening during starvation. The biofilms are rheologically inhomogeneous on the micron scale, as a result of the strength of initial adhesion to the flow cell surface, the arrangement of individual bacteria, and larger-scale structures such as flocs of *P. aeruginosa*. Our *S. aureus* biofilms became homogeneous as a function of height as they matured: the rheological environment experienced by a bacterium became independent of how far it lived from the flow cell surface.

Our study has shown that PTM provides a quantitative measure of the "strength" of a biofilm, which is measured noninvasively on the micron scale in different locations of the Biofilm. The results of PTM are relevant to diffusion within the biofilm, attack by phagocytic cells, and dispersal of the biofilm; therefore PTM may prove useful in identifying drug targets.

Acknowledgment. This work was supported by the U.K. Medical Research Council, grant reference 80360. We would like to thank Dr. Alex Dajkovic and Dr. Paul Herron for their helpful discussions. We also thank Dr. Paul Herron for his critical reading of the manuscript.

Supporting Information Available: Time lapse videos of *S. aureus* and *P. aeruginosa*. This material is available free of charge via the Internet at http://pubs.acs.org.

LA802442D